

# Controlled Anionic Graft Polymerization of Ethylene Oxide Directly from Poly(*N*-isopropylacrylamide)

Junpeng Zhao and Helmut Schlaad\*

Department of Colloid Chemistry, Max Planck Institute of Colloids and Interfaces, Research Campus Golm, 14424 Potsdam, Germany

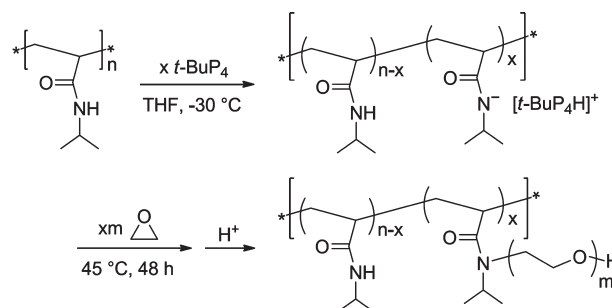
Graft copolymers with poly(ethylene oxide) (PEO) side chains have been of great interest in both academia and industry<sup>1</sup> due to some desirable properties brought in by the branched macromolecular architecture, such as extended chain conformation and low inherent viscosity, and by PEO side chains, such as water solubility, crystallinity, biocompatibility, and protein/cell resistance.<sup>2,3</sup> Among all PEO-bearing graft copolymers, the ones having poly(*N*-isopropylacrylamide), PNIPAM, as the backbone have received considerable attention. PNIPAM is the most studied thermoresponsive polymer with a lower critical solution temperature (LCST) in water at 32 °C, and for its graft copolymer with PEO (PNIPAM-*g*-PEO), the molecular structure and the persistent hydrophilicity of the side chains can be utilized to modulate the responsiveness in terms of LCST and structure of the aggregates.<sup>4–7</sup> It has been found that with certain molecular characteristics and experimental conditions this graft copolymer shows some extraordinary thermoresponsive behaviors such as the reversible single chain “coil-to-globule” transition giving rise to single chain core–shell nanostructures.<sup>6,7</sup>

For a better modulation of the properties of PEO-based graft copolymers, synthetic methodologies have been developed for controlling molecular weight, composition, side chain length, and distribution.<sup>1,4–13</sup> Nevertheless, the preparation of PNIPAM-*g*-PEO has achieved quite limited development. To our knowledge, two conventional methods have been involved so far, namely, the coupling of end-functionalized PEO onto PNIPAM with reactive moieties (“grafting onto”)<sup>4,5</sup> and the copolymerization of NIPAM with PEO macromonomer (“grafting through”).<sup>6,7</sup> However, from a chemical point of view, neither of these two methods can achieve absolutely random distribution of PEO chains along the backbone. Moreover, the varieties of side chain lengths and graft densities are also quite limited. Therefore, we attempted to develop a new method toward PNIPAM-*g*-PEO graft copolymer with better controlled molecular structure.

The graft polymerization of ethylene oxide (EO) from backbones with multifunctional initiating sites has been employed quite often.<sup>9–13</sup> Such a “grafting from” technique is able to achieve a better control of the synthesis and a wide variety of molecular characteristics compared to the other two techniques mentioned above. The main disadvantages are the use of metal-based catalysts as well as the necessity of incorporating functional moieties into the backbone polymer,<sup>9–11</sup> which inevitably inflicts complexity on the synthetic procedures and doubt about the randomness of the side chain distribution.

It is known that amide moieties in the backbone polymer can be deprotonated by a strong base, thus generating anionic initiating sites to polymerize EO.<sup>11,12</sup> In our previous work, the

**Scheme 1. Synthetic Scheme for the Direct Growth of PEO Side Chains from PNIPAM by Metal-Free Anionic Graft Polymerization**



phosphazene base, *t*-BuP<sub>4</sub>, has opened a new pathway to PEO-based linear and graft copolymers via metal-free anionic polymerization.<sup>13,14</sup> Therefore, we were inspired to take advantage of both *t*-BuP<sub>4</sub> and secondary amide moieties in PNIPAM, so as to create anionic initiating sites and grow PEO directly from PNIPAM backbone (Scheme 1). By this approach, the synthesis of PNIPAM-*g*-PEO would be greatly simplified since the introduction of functional moieties is avoided. Moreover, the molecular structure, in terms of molecular composition and graft density of the graft copolymer, could be controlled.

PNIPAM, with an apparent number-average molecular weight ( $M_n^{app}$ ) of 43 kg/mol and a polydispersity index (PDI) of 1.13, as determined by size-exclusion chromatography (SEC), was prepared by reversible addition–fragmentation chain transfer (RAFT) polymerization using 3-benzylsulfanylthiocarbonylsulfanylpropionic acid (BPATT) as the chain transfer agent.<sup>15</sup> PNIPAM was subsequently subjected to reaction with excess 2,2′-azobis(isobutyronitrile) (AIBN) to remove the 2-carboxyethylsulfanylthiocarbonylsulfanyl end group,<sup>16</sup> which would be unfavorable for the anionic graft polymerization. Before each graft polymerization, PNIPAM was thoroughly dried by three azeotropic distillations of tetrahydrofuran (THF, dried by Na/K alloy) and high vacuum.

A certain amount of *t*-BuP<sub>4</sub> (1 M in *n*-hexane) solution was added to the THF solution of PNIPAM, giving desired [*t*-BuP<sub>4</sub>]<sub>0</sub>/[NIPAM]<sub>0</sub> ratio (Scheme 1 and Table 1), where

**Received:** June 1, 2011

**Revised:** July 9, 2011

**Published:** July 15, 2011

**Table 1.** Molecular Characteristics of PNIPAM-*g*-PEO Graft Copolymers

sample	$[t\text{-BuP}_4]_0/[\text{NIPAM}]_0$	$\Delta(\text{amide II/I})^a$	PDI <sup>b</sup>	$M_n^{\text{app } c}$ (kg/mol)	$w_{\text{PEO}}^d$	$M_{n,\text{PEO}}^e$ (kg/mol)
PNIPAM			1.13	43		
NGE1	0.012	0.011	1.21	47	0.09	1.1
NGE2	0.023	0.022	1.25	60	0.28	2.0
NGE3	0.053	0.060	1.21	81	0.47	1.9
NGE4	0.100	0.120	1.19	126	0.66	2.1

<sup>a</sup> From FT-IR analysis. <sup>b</sup> Determined by SEC. <sup>c</sup> Calculated from  $M_n^{\text{app}}$  of PNIPAM and  $^1\text{H}$  NMR integrals. <sup>d</sup> Weight fraction of PEO in each NGE graft copolymer calculated from  $^1\text{H}$  NMR integrals. <sup>e</sup> Average molecular weight of PEO side chains estimated as  $M_{n,\text{PEO}} = fM_{\text{EO}}/([t\text{-BuP}_4]_0/[\text{NIPAM}]_0)$ , where  $f$  and  $M_{\text{EO}}$  denote the molar ratio of EO to NIPAM repeat units (determined by  $^1\text{H}$  NMR integrals) and molecular weight of EO repeat unit, respectively.

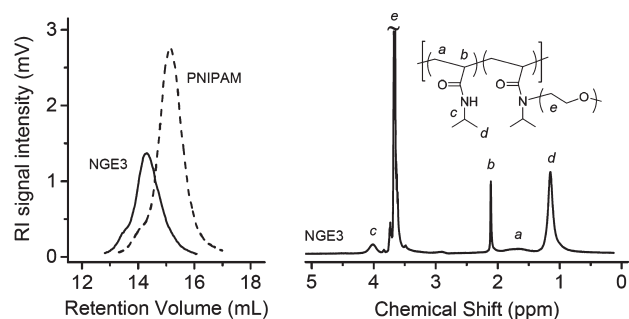


**Figure 1.** (left) SEC traces of PNIPAM and a representative PNIPAM-*g*-PEO copolymer (sample NGE3, Table 1), with the same concentration of the injected solutions (1.5 mg/mL). (right)  $^1\text{H}$  NMR spectrum (400.1 MHz,  $\text{CDCl}_3$ ) of NGE3.

$[\text{NIPAM}]_0$  denotes the initial molar concentration of PNIPAM repeat units (or the secondary amide moieties). The PNIPAM solution turned yellowish immediately upon addition of  $t\text{-BuP}_4$ , indicating the occurrence of deprotonation and the generation of anions. The deprotonation of primary and secondary amide moieties in a polymer backbone by potassium *tert*-butoxide was proven to be effective.<sup>11,12</sup> Considering the much higher basicity,<sup>17</sup> we expected that the deprotonation of NIPAM units with  $t\text{-BuP}_4$  would be quantitative.

After the cryo-condensation of a predetermined amount of EO, the reactor was sealed by a stopcock, and polymerization was conducted at 45 °C for 48 h. The yellow color of the solution disappeared right upon quenching with acetic acid. The graft copolymers, herein termed as NGE1–4, were isolated by dialysis followed by freeze-drying. With lower PEO weight fraction ( $w_{\text{PEO}}$ , Table 1) the isolated copolymer samples still remained solid (NGE1, 2), while those with higher  $w_{\text{PEO}}$  appeared to be syrupy (NGE3, 4), which gives a visual indication of the graft molecular structure. SEC traces of the products clearly showed the increase in molecular weight after graft polymerization (Figure 1, left), and that all NGE graft copolymers were narrowly distributed (PDI  $\sim$  1.2, Table 1).

It is important to note that the polymerization of EO did not occur with poly(*N,N*-dimethylacrylamide) (PDMAM)/ $t\text{-BuP}_4$ , as indicated by SEC (not shown). Since PDMAM consists of tertiary amide moieties and no NH protons, it could be inferred that all the other protons (backbone protons and  $\text{N}(\text{CH}_3)_2$  protons) were not acidic enough to be deprotonated and converted into initiating sites. Hence, it could be concluded that in the case of PNIPAM only the secondary amide moieties participated in the deprotonation and initiation steps.

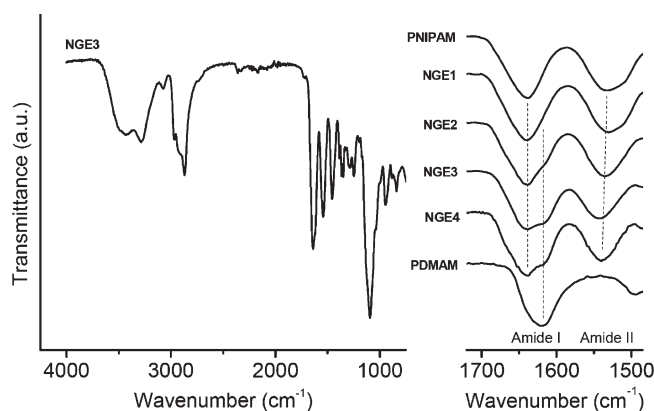


**Figure 2.** FT-IR spectra of PNIPAM-*g*-PEO copolymer NGE3 (left) and expanded region of amide I and amide II bands of NGE1–4, PNIPAM, and PDMAM reference samples (right).

The yield of each graft polymer was higher than 90%. Because of the possible loss of material during purification, however, accurate molecular weights might not be obtained by calculation based on yield. The  $^1\text{H}$  NMR spectrum of a representative graft copolymer sample (NGE3) is displayed in Figure 1 (right), showing all the characteristic peaks of both PNIPAM and PEO. The integrals of peaks assigned to NCH in PNIPAM and methylene protons in PEO (peaks *c* and *e* in Figure 1) were used to calculate the molecular weight as well as  $w_{\text{PEO}}$  of each sample (Table 1). All of these values were quite close to the theoretical ones, as calculated by the feed ratio (not shown) in each graft polymerization, which indicated the nearly complete conversion of EO.

The molecular structure of NGE graft copolymers was also characterized by Fourier transform infrared spectroscopy (FT-IR). The characteristic absorption bands of PNIPAM (1485–1680  $\text{cm}^{-1}$ , amide region) and PEO (1100  $\text{cm}^{-1}$ , C–O stretching) were clearly presented in the spectra of the graft copolymers (Figure 2), which further confirmed the successful growth of PEO side chains. A distinct C=N absorption band (1600–1700  $\text{cm}^{-1}$ ) could not be clearly identified, suggesting that all PEO chains were linked to the PNIPAM backbone via the amide nitrogen atom, as depicted in Scheme 1 and Figure 1, and not via the oxygen (as to be expected considering the resonance structure of the amide anion).<sup>18</sup> The signals of the amide I (1580–1680  $\text{cm}^{-1}$ ) and amide II (1485–1580  $\text{cm}^{-1}$ ) bands, which were mostly contributed by C=O stretching and N–H bending, respectively, were analyzed in greater detail (Figure 2, right).<sup>19</sup> Since the deprotonation and

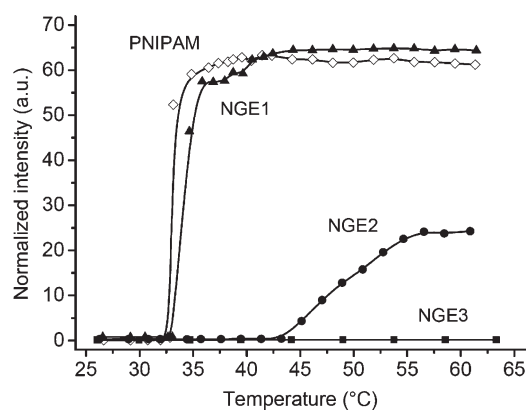


**Figure 3.** Temperature dependence of average scattering intensity at 90° of PNIPAM precursor and PNIPAM-g-PEO copolymer samples NGE1–3 in aqueous solution (concentration: 1 mg/mL).

growth of PEO chains converted a certain amount of secondary amide moieties into tertiary amide, the intensity ratio of amide II to amide I (amide II/I) given by the graft copolymer would decrease compared to that of PNIPAM. Tertiary amides lack the amide II band, as evidenced by the FT-IR spectrum of PDMAM (Figure 2, right). Therefore, using the amide II/I of PNIPAM and each graft copolymer, we could estimate the decrease of amide II/I, termed as  $\Delta(\text{amide II/I})$  (Table 1). Here we are not able to prove that  $\Delta(\text{amide II/I})$  is equal to the graft density (the percentage of NIPAM repeat units grafted with PEO), but it is still reasonable to consider it as a good reflection of the graft density. It has to be noted that amide II/I ratios were calculated by the maximum absorbance of each peak; integrals were not used because of the profound overlap of peaks.

It was found that the  $\Delta(\text{amide II/I})$  values of the NGE samples were quite close to the corresponding  $[t\text{-BuP}_4]_0/[\text{NIPAM}]_0$  ratios, suggesting that graft density was greatly dependent on or related to  $[t\text{-BuP}_4]_0/[\text{NIPAM}]_0$ . It is therefore concluded that the deprotonation of NIPAM units by  $t\text{-BuP}_4$  was quantitative and, furthermore, that chain transfer from the growing PEO chains to nonreacted secondary amide moieties on the backbone was hardly taking place. This result is rather surprising considering the  $pK_a$  values of primary alcohols (ethanol,  $pK_a = 29.8$  in DMSO)<sup>20a</sup> and amides (*N*-methylacetamide,  $pK_a = 25.9$  in DMSO),<sup>20b</sup> according to which secondary amides should be readily deprotonated by alcoholates (see also Wesslén et al.,<sup>11,12</sup> vide supra). Suppression of chain transfer may be due to steric hindrance of the secondary amide moieties, thus allowing to control the graft density in the investigated range of  $[t\text{-BuP}_4]_0/[\text{NIPAM}]_0 \leq 0.1$ .

It could be seen in Figure 2 that a shoulder existed in the amide I band of each NGE sample, with the wavelength of maximum absorbance very close to that of the amide I of PDMAM. This further evidenced that some of the secondary amide moieties were turned into tertiary amide. As  $[t\text{-BuP}_4]_0/[\text{NIPAM}]_0$  increased (from NGE1 to NGE4), the shoulder became more and more intensive, which could be a possible reason why  $\Delta(\text{amide II/I})$  of NGE3 and NGE4 was slightly higher than the corresponding  $[t\text{-BuP}_4]_0/[\text{NIPAM}]_0$ . Therefore,  $[t\text{-BuP}_4]_0/[\text{NIPAM}]_0$  might better reflect the true graft density, and the average molecular weight of PEO side chains,  $M_{n,\text{PEO}}$ , could be estimated from the values of  $w_{\text{PEO}}$  and  $[t\text{-BuP}_4]_0/[\text{NIPAM}]_0$  (Table 1). In this case, both the graft

density and side chain length are independent of the length of PNIPAM backbone.

The thermoresponsive behaviors of the NGE samples were briefly investigated by light scattering. Figure 3 shows the temperature dependence of average scattering intensity given by NGE samples, compared with PNIPAM precursor, in dilute aqueous solution (1 mg/mL). NGE3, with 47 wt % of PEO, did not show any increase in scattering intensity up to ca. 63 °C (also observed for NGE4). However, for linear PNIPAM-*b*-PEO block copolymers with the similar PEO weight fraction, this temperature is high enough to bring about aggregation, though to a relatively low extent.<sup>21–23</sup> This was probably because PEO side chains segregated the PNIPAM backbones into short segments and could better stabilize the collapsed graft copolymer.<sup>3,5</sup> The NGE samples with lower  $w_{\text{PEO}}$  (NGE1, 2) presented significant aggregation at elevated temperature (Figure 3). Higher aggregation temperature and lower scattering intensity given by the aggregates were observed for NGE2 containing a higher fraction of PEO. This first light scattering study revealed the structure-related thermoresponsive behavior and further confirmed the graft molecular structure of the polymers. A detailed analysis of the aggregation behavior of NGE copolymers by light scattering is currently being performed.

In summary, we have introduced a facile synthetic approach toward PNIPAM-PEO graft copolymers by using  $t\text{-BuP}_4$  to deprotonate the secondary amide moieties in PNIPAM and subsequently growing PEO chains anionically. It has been evidenced that the graft density depended greatly on  $[t\text{-BuP}_4]_0/[\text{NIPAM}]_0$ . Therefore, by varying the feed ratio of  $t\text{-BuP}_4$ , PNIPAM, and EO, a wide range of molecular structures, with tunable thermoresponsive behavior, could be obtained. This method could probably be extended to other monomers, such as other epoxides or lactones, as well as to other backbone polymers with secondary amide moieties, such as polypeptides, polyamides, etc., for the generation of a toolbox of novel “smart” copolymers.

## EXPERIMENTAL SECTION

**Chemicals.** NIPAM (99%, Aldrich) was recrystallized from toluene/*n*-hexane (1:4 v/v); 4,4'-azobis(4-cyanovaleric acid) (ACVA) (98%, Aldrich) and AIBN (98%, Aldrich) were recrystallized from methanol. BPATT was kindly donated by Axel H. E. Müller group. Phosphazene base,  $t\text{-BuP}_4$  (Aldrich, 1 M solution in *n*-hexane), was used as received. For RAFT polymerization and end-group removal, acetone (p.a. Baker), THF, and diethyl ether (p.a., VWR) were used as received; for anionic graft polymerization, THF was dried successively by Na and Na/K alloy. EO (99.8%, Aldrich) was dried successively by  $\text{CaH}_2$  and *n*-butyllithium (twice) prior to graft polymerization.

**Polymer Synthesis.** **PNIPAM.** NIPAM (10.0 g), BPATT (65.7 mg), and ACVA (6.7 mg) were dissolved in 20 mL of water/acetone (1:1 v/v); after three freeze–pump–thaw cycles, the solution was heated at 60 °C for 3 days. After quenching with rapid cooling, acetone was evaporated, and the residual solution of PNIPAM was dialyzed in cellulose membrane (molecular weight cutoff: 3.5 kg/mol) against distilled water for 3 days. After freeze-drying, 9.65 g of PNIPAM was obtained. Subsequently, PNIPAM (9.65 g) and AIBN (0.39 g) was dissolved in 30 mL of THF, and after three freeze–pump–thaw cycles, the solution was heated at 60 °C for 24 h to remove the end-group. PNIPAM was isolated by precipitation in cold diethyl ether three times and



dried under vacuum. SEC:  $M_n^{\text{app}} = 43$  kg/mol, PDI = 1.13. PDMAM. See PNIPAM. SEC:  $M_n^{\text{app}} = 35$  kg/mol, PDI = 1.10. PNIPAM-*g*-PEO. Typical procedure (NGE3): 2.0 g of PNIPAM was dissolved in ~20 mL of dry THF, followed by slow cryo-evaporation of THF. After repeating this step three times, PNIPAM was dried thoroughly on vacuum line overnight with constant pumping. The next day, another 40 mL of dry THF was condensed into the reactor. After complete dissolution of PNIPAM, 0.93 mL of *t*-BuP<sub>4</sub> solution (1 M) was added dropwise with an argon flow. The solution was stirred for 30 min, and temperature was brought down to -30 °C, after which 2.3 mL of purified EO (~2.0 g) was condensed slowly into the reactor. Then the reactor was sealed by a stopcock, and temperature was slowly raised to 45 °C, at which the solution was heated and stirred for 48 h. The polymerization was quenched by 0.2 mL of acetic acid. After evaporation of THF, the crude product was dissolved in distilled water and dialyzed for 3 days (molecular weight cutoff: 3.5 kg/mol). Finally, the pure graft copolymer was obtained after freeze-drying. Yield: 90%. SEC: PDI = 1.21. <sup>1</sup>H NMR (400.1 MHz, CDCl<sub>3</sub>):  $\delta$ /ppm = 4.0 (-CONHCH(CH<sub>3</sub>)<sub>2</sub>), 3.8–3.2 (-OCH<sub>2</sub>CH<sub>2</sub>-), 2.3–0.8 (CH<sub>2</sub>CHCO and -CONHCH(CH<sub>3</sub>)<sub>2</sub>);  $M_n^{\text{app}} = 81$  kg/mol.

**Instrumentation.** SEC with simultaneous UV and RI detection was conducted in *N*-methyl-2-pyrrolidone (NMP + 0.5 wt % LiBr) at 70 °C using a column set of two 300 × 8 mm<sup>2</sup> PSS-GRAM (7 μm) columns with porosities of 10<sup>2</sup> and 10<sup>3</sup> Å, respectively. Calibration was done with polystyrene standards (PSS GmbH). <sup>1</sup>H NMR measurements were carried out at room temperature using a Bruker DPX-400 spectrometer operating at 400.1 MHz; CDCl<sub>3</sub> (Aldrich) was used as solvent. FT-IR spectra were recorded on a BioRad 6000 FT-IR spectrometer; samples were measured in solid state using a Single Reflection Diamond ATR. Light scattering was measured using a goniometer setup at scattering angle 90°. The instrument is equipped with a HeNe laser (Polytec, 34 mW,  $\lambda = 633$  nm), a digital correlator (ALV 5000), and a photon detector (ALV/SO-SIPD).

## AUTHOR INFORMATION

### Corresponding Author

\*Fax: +49(0)331.567.9502. E-mail: schlaad@mpikg.mpg.de.

## ACKNOWLEDGMENT

We thank Jessica Brandt, Marlies Gräwert, Nora Fiedler, and Olaf Niemeyer for helping hands and technical assistance. Yusuf Yagci is thanked for a great time and critical reading of the manuscript. Financial support was given by the Max Planck Society.

## REFERENCES

- (1) (a) Neugebauer, D. *Polym. Int.* **2007**, *56*, 1469–1498. (b) Xie, H.-Q.; Xie, D. *Prog. Polym. Sci.* **1999**, *24*, 275–313.
- (2) (a) Ali, M. M.; Stöver, H. D. H. *Macromolecules* **2004**, *37*, 5219–5227. (b) Lutz, J.-F.; Hoth, A. *Macromolecules* **2006**, *39*, 893–896. (c) Hester, J. F.; Banerjee, P.; Won, Y.-Y.; Akthakul, A.; Acar, M. H.; Mayes, A. M. *Macromolecules* **2002**, *35*, 7652–7661. (d) Ishizone, T.; Han, S.; Hagiwara, M.; Yokoyama, H. *Macromolecules* **2006**, *39*, 962–970. (e) Neugebauer, D.; Zhang, Y.; Pakula, T.; Sheiko, S. S.; Matyjaszewski, K. *Macromolecules* **2003**, *36*, 6746–6755. (f) Yokoyama, H.; Miyamae, T.; Han, S.; Ishizone, T.; Tanaka, K.; Takahara, A.; Torikai, N. *Macromolecules* **2005**, *38*, 5180–5189.

- (3) (a) Xu, P.; Tang, H.; Li, S.; Ren, J.; Van Kirk, E.; Murdoch, W. J.; Radosz, M.; Shen, Y. *Biomacromolecules* **2004**, *5*, 1736–1744. (b) Robinson, D. N.; Peppas, N. A. *Macromolecules* **2002**, *35*, 3668–3674. (c) Zhang, R.; Seki, A.; Ishizone, T.; Yokoyama, H. *Langmuir* **2008**, *24*, 5527–5533. (d) Oyane, A.; Ishizone, T.; Uchida, M.; Furukawa, K.; Ushida, T.; Yokoyama, H. *Adv. Mater.* **2005**, *17*, 2329–2332.
- (4) Virtanen, J.; Baron, C.; Tenhu, H. *Macromolecules* **2000**, *33*, 336–341.
- (5) Virtanen, J.; Tenhu, H. *Macromolecules* **2000**, *33*, 5970–5975.
- (6) Qiu, X.; Wu, C. *Macromolecules* **1997**, *30*, 7921–7926.
- (7) Wu, C.; Qiu, X. *Phys. Rev. Lett.* **1998**, *80*, 620–622.
- (8) (a) Neugebauer, D.; Zhang, Y.; Pakula, T.; Matyjaszewski, K. *Macromolecules* **2005**, *38*, 8687–8693. (b) Han, S.; Hagiwara, M.; Ishizone, T. *Macromolecules* **2003**, *36*, 8312–8319. (c) Wang, X.-S.; Armes, S. P. *Macromolecules* **2000**, *33*, 6640–6647. (d) Yuan, W.; Yuan, J.; Zhang, F.; Xie, X.; Pan, C. *Macromolecules* **2007**, *40*, 9094–9102.
- (9) Se, K.; Miyawaki, K.; Hirahara, K.; Takano, A.; Fujimoto, T. *J. Polym. Sci., Part A: Polym. Chem.* **1998**, *36*, 3021–3034.
- (10) Lanson, D.; Schappacher, M.; Borsali, R.; Deffieux, A. *Macromolecules* **2007**, *40*, 9503–9509.
- (11) Jannasch, P.; Wesslén, B. *J. Polym. Sci., Part A: Polym. Chem.* **1993**, *31*, 1519–1529.
- (12) Dérand, H.; Jannasch, P.; Wesslén, B. *J. Polym. Sci., Part A: Polym. Chem.* **1998**, *36*, 803–811.
- (13) (a) Zhao, J.; Mountrichas, G.; Zhang, G.; Pispas, S. *Macromolecules* **2009**, *42*, 8661–8668. (b) Zhao, J.; Mountrichas, G.; Zhang, G.; Pispas, S. *Macromolecules* **2010**, *43*, 1771–1777.
- (14) (a) Schlaad, H.; Kukula, H.; Rudloff, J.; Below, I. *Macromolecules* **2001**, *34*, 4302–4304. (b) Groenewolt, M.; Brezesinski, T.; Schlaad, H.; Antonietti, M.; Groh, P. W.; Iván, B. *Adv. Mater.* **2005**, *17*, 1158–1162.
- (15) (a) Stenzel, M. H.; Davis, T. P. *J. Polym. Sci., Part A: Polym. Chem.* **2002**, *40*, 4498–4512. (b) Millard, P.-E.; Barner, L.; Stenzel, M. H.; Davis, T. P.; Barner-Kowollik, C.; Müller, A. H. E. *Macromol. Rapid Commun.* **2006**, *27*, 821–828.
- (16) Perrier, S.; Takopuckdee, P.; Mars, C. A. *Macromolecules* **2005**, *38*, 2033–2036.
- (17) Memeger, W.; Campbell, G. C. C.; Davidson, F. *Macromolecules* **1996**, *29*, 6475–6480.
- (18) Ito, M.; Ishizone, T. *J. Polym. Sci., Part A: Polym. Chem.* **2006**, *44*, 4832–4845.
- (19) Sun, S.; Wu, P. *Macromolecules* **2010**, *43*, 9501–9510.
- (20) (a) Olmstead, W. N.; Margolin, Z.; Bordwell, F. G. *J. Org. Chem.* **1980**, *45*, 3295–3299. (b) Bordwell, F. G.; Harrelson, J. A.; Lynch, T. Y. *J. Org. Chem.* **1990**, *55*, 3337–3341.
- (21) Zhang, W.; Shi, L.; Wu, K.; An, Y. *Macromolecules* **2005**, *38*, 5743–5747.
- (22) Zhu, K.; Pamies, R.; Kjøniksen, A.-L.; Nyström, B. *Langmuir* **2008**, *24*, 14227–14233.
- (23) Motokawa, R.; Morishita, K.; Koizumi, S.; Nakahira, T.; Annaka, M. *Macromolecules* **2005**, *38*, 5748–5760.